Ss. Cyril and Methodious University
Faculty of Electrical Engineering and Information
Technology
Institute of Telecommunications
Skopje, Macedonia

Jovan Stosic

Cooperative Communications over Wireless Relay Channels

- Abstract of Ph.D. Thesis -

Supervisor: Prof. Dr. Zoran Hadzi-Velkov

Skopje, 2014

Ss. Cyril and Methodious University
Faculty of Electrical Engineering and Information Technology
Institute of Telecommunications
Skopje, Macedonia

Jovan Stosic

Cooperative Communications over Wireless Relay Channels

- Ph. D. Thesis -

Abstract

Cooperative (relay) communications is a very important research area of the wireless communications [1]. Its concept is based upon the properties of the wireless channel, i.e. the multi-path propagation which can be utilized to increase the efficiency and the robustness of the communications system. Adjacent wireless nodes (also known as relays or partners) are helping each other in the process of communication by dedicating part of their resources for transmission of a part or all data from the partner.

In the thesis we analyze the cooperative relay channel from information-theoretic and communication-theoretic perspective, including both the single-input single-output (SISO) relay channel and the multiple-input multiple-output (MIMO) relay channel. For the SISO relay channel, we study the capacity upper bound of the relay channel, as well as bounds on the achievable rates of the main relaying schemes ([2], [3]).

For the MIMO relay channel, we focus on the two-hop MIMO relay channels with orthogonal space-time block coding (OSTBC) in Rayleigh fading environment. We assume that the relay is using a special type of amplify-and-forward (AF) scheme [4], called the Decouple-and-Forward (DCF) [5]. The full channel state information (CSI) is available to both the relay and destination. In AF relay, the input signal is decoupled, amplified and forwarded toward the destination. For such setup, we derive tight and loose error probability (EP) approximations for the entire signal-to-noise (SNR) region of practical interest. In the high SNR regions, the tight approximations are simplified into simple asymptotic EP expressions. The obtained EP approximations are compared with the EP obtained by applying the moment generating function (MGF) method, as well as by computer Monte Carlo simulations. We also derive similar approximations for the outage probability (OP) for the considered AF relaying scheme. The OP approximations are compared with the exact results obtained from the numerical integration based on the MGF and from computer Monte Carlo simulations. Additionally we derive closed form OP approximation of AF MIMO relay channel with direct path to the destination. Finally, we derive expressions for the ergodic capacity and outage capacity of the AF MIMO relay channel with and without direct path to the destination. The systems with direct path significantly outperform the systems without direct path in terms of ergodic capacity and outage capacity.

1   Capacity of Cooperative Relay Channels

In this chapter, we present the derivations for the bounds of the achievable rates for the most important relaying schemes: Decode-and-Forward (DF) Gaussian relay channel, Compress-and-Forward (CF) Gaussian relay channel and Amplify-and-Forward (AF) Gaussian relay channel.

These expressions are already known in the literature, however we re-derive these capacity expressions by including our own original derivation steps. These derivations are fitted to the communication-theoretic analysis in the successive chapters. We analyze the cooperative relay system with three nodes [6] which is represented with Fig. 1. The source (node 1) wants to communicate the message W with the destination (node 3) with help of the relay (node 2). We analyze discrete memoryless relay channel (DMRC) which is denoted with: $(X_1 \times X_2, p(y_2, y_3 | x_1, x_2), Y_2 \times Y_3)$, consisted of four finite sets X_1, X_2, Y_2, Y_3, and conditional probability $p(y_2, y_3 | x_1, x_2)$ of set $Y_2 x Y_3$ for each $(x_1, x_2) \in X_1 x X_2$, where x_1 is a transmitted signal at the source, y_2 is the received signal at the relay, y_3 is the received signal at the destination, and x_2 is the transmitted signal at the relay. The code $(2^{nR}, n)$ for DMRC consist of: set of messages $\left[1 : 2^{nR} \right]$, encoder which assigns the codeword $x_1^n(w)$ to each message $w \in [1 : 2^{nR}]$, encoder in the relay which assigns symbol $x_{2i}(y_2^{i-1})$ to each previously received sequence $y_2^{i-1} \in Y_2^{i-1}$ for each time $i \in [1 : n]$ and a decoder in the destination that assigns an estimate $\hat{w}$ or an error e to each received sequence $y_3^n \in Y_3^n$. The channel is memoryless in the sense that the current received symbols (Y_2^i, Y_3^i) and the messages and past symbols $(w, X_1^{i-1}, X_2^{i-1}, Y_2^{i-1}, Y_3^{i-1})$ are conditionally independent given the current transmitted symbols (X_1^i, X_2^i). Although the capacity of the general relay channel is unknown, there are several special cases for which the capacity has been established: (a) the physically degraded and the reversely degraded relay channels [2], (b) the semi-deterministic relay channel [7], (c) the orthogonal relay channel [8], and (d) a class of deterministic relay channels [9]. Therefore, in the systems where the capacity cannot be exactly found we analyze the upper and lower capacity bounds. As one of the most important and practical cases of relay channel, the Gaussian relay channel has been thoroughly analyzed with emphasis on the DF, CF and AF relaying schemes.
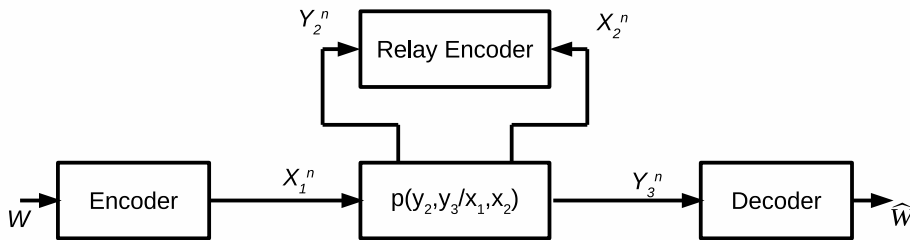
Figure 1: Point to point communication system with relay

## 1.1 Capacity of main relay processing schemes

In general the upper capacity bound of DMRC is:

$$C \leq \max_{p(x_1 x_2)} \min \left\{ I\left(X_1, X_2; Y_3\right), I\left(X_1; Y_2, Y_3 | X_2\right) \right\} . \tag{1}$$

This bound is called cutset upper bound (CUB) since the elements of the minimum may be interpreted as cooperative combination of multiple-access channel [10, ch.(15.3)] and broadcast channel [10, ch.(15.6)] which is illustrated on Fig. 2. CUB is information-theoretic generalization of the maximal flow - minimal cut theorem [11].

One simple scheme for coding of the relay channel is *direct transmission* for which the lower capacity bound is [3, ch.(16.3)]:

$$C_{DT} \geq \max_{x_2 \in X} \max_{p(x_1)} I(X_1; Y_3 | x_2) . \tag{2}$$

Cooperative multiple access bound   Cooperative broadcast bound
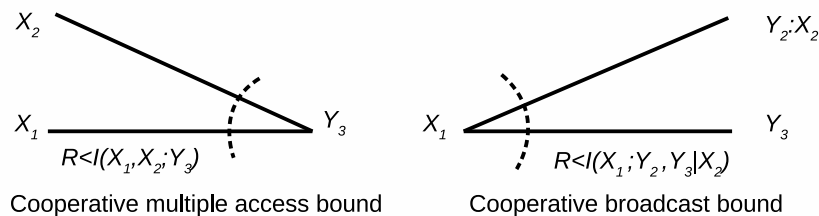
Figure 2: Interpretation of the cutset upper bound with maximal flow-minimal cut theorem

In the two-hop *cascade relay channel*, the relay is reconstructing the message received form the source in each block and retransmitting it in the next block (Fig. 3). Since the codeword sent by the relay is statistically dependent form the message sent in the previous block, this type of coding is called block Markov coding (BMC) [12]. The lower bound of the capacity of this system is:

$$C \geq \max_{p(x_1)p(x_2)} \min\left\{I\left(X_2;Y_3\right), I\left(X_1;Y_2|X_2\right)\right\} = \min\left\{\max_{p(x_2)}\left\{I\left(X_2;Y_3\right)\right\}, \max_{p(x_1)}\left\{I\left(X_1;Y_2\right)\right\}\right\}.$$

(3)

The rate achieved in the two-hop cascade relay channel may be improved if we allow the
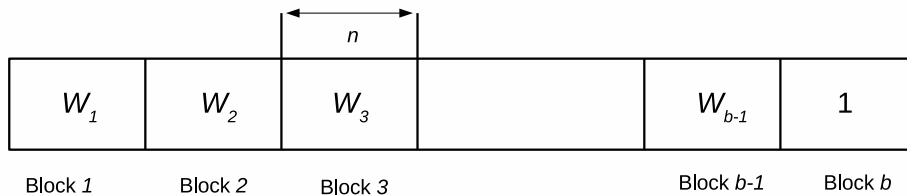
Figure 3: Set of transmission blocks used in two-hop cascade relay channel

source and the relay to coherently collaborate in the sending of their codewords. With this improvement we get the lower bound of the capacity of the *coherent cascade* relay channel:

$$C \geq \max_{p(x_1,x_2)} \min\left\{I\left(X_2;Y_3\right), I\left(X_1;Y_2|X_2\right)\right\}.$$

(4)

We again use BMC in which the $(b-1)$ i.i.d messages W_j, $j \in [1:b-1]$ are sent over b blocks where each block is transmitted by n accesses to the channel.

The capacity performance of the cascade relay channel may be improved if the destination is simultaneously decoding the messages sent from the source and the relay. With this improvement we get *Decode-and-Forward* relay channel with lower capacity bound:

$$C \geq \max_{p(x_1 x_2)} \min\left\{I\left(X_1 X_2;Y_3\right), I\left(X_1;Y_2|X_2\right)\right\},$$

(5)

where (5) can be proved by usage of random binning ([13],[3]).

Degraded relay channel is DMRC where the received signal in the relay y_2 is better than the signal in the destination y_3. The relay channel $(X_1 \mathrm{x} X_2, p(y_3, y_2|x_1, x_2), Y_2 \mathrm{x} Y)$ is called *degraded* if $p(y_3, y_2|x_1, x_2)$ may be written in following form:

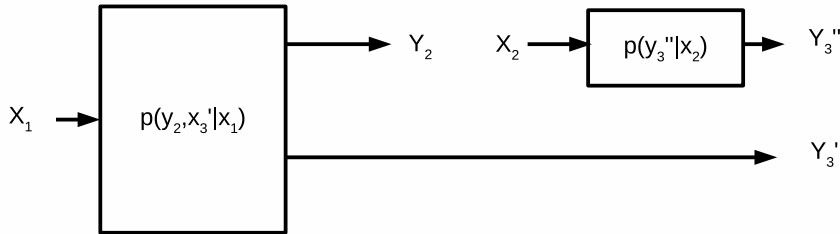$$p(y_3, y_2|x_1, x_2) = p(y_2|x_1, x_2) \cdot p(y_3|y_2, x_2).$$

(6)

From (6) follows that relay channel is degraded if $p(y_3|x_1, x_2, y_2) = p(y_3|x_2, y_2)$ i.e., $X_1 \rightarrow (X_2, Y_2) \rightarrow Y_3$ form Markov chain [10, eq.(2.117)]. The capacity of the degraded relay channel is:

3

$$C = \max_{p(x1,x2)} \min \left\{ I(X_1, X_2; Y_3), I(X_1; Y_2|X_2) \right\} . \tag{7}$$

In the DF relaying scheme, the relay recovers the entire message. If the channel from the source to the relay is weaker than the direct channel to the destination, this requirement can reduce the rate below that for direct transmission in which the relay is not used at all. In the *Compress-and-Forward* relaying scheme the relay helps communication by sending a description of its received sequence to the receiver. Since this description is correlated with the received sequence, Wyner-Ziv coding [14] is used to reduce the rate needed to communicate it to the destination. This scheme achieves the following lower bound:

$$C \geq \max \min \left\{ I\left(X_1, X_2; Y_3\right) - I\left(Y_2; \hat{Y}_2|X_1 X_2 Y_3\right), I\left(X_1; \hat{Y}_2, Y_3|X_2\right) \right\} . \tag{8}$$

Subtype of the CF relay channel is the DMRC with orthogonal receiver components (ORC) depicted in Fig. 4:

Figure 4: Relay channel with orthogonal receiver components

Here $Y_3 = (Y_3', Y_3'')$ and $p\left(y_2, y_3|x_1 x_2\right) = p\left(y_3', y_2|x_1\right) p\left(y_3''|x_2\right)$, decoupling the broadcast channel form the source to the relay and the destination form the direct channel from the relay to the destination. The capacity of the DMRC with orthogonal receiver components is not known in general. The CUB (1) for ORC relay channel simplifies to:

$$C \leq \max_{p(x_1)p(x_2)} \min \left\{ I\left(X_1; Y_3'\right) + I\left(X_2; Y_3''\right), I\left(X_1; Y_2, Y_3'\right) \right\} . \tag{9}$$

1.2 Capacity of Gaussian relay channel

Consider the Gaussian relay channel depicted on Fig. 5, which is a simple model for wireless point-to-point communication with a relay [3]. The channel outputs corresponding to the inputs X_1 and X_2 are:
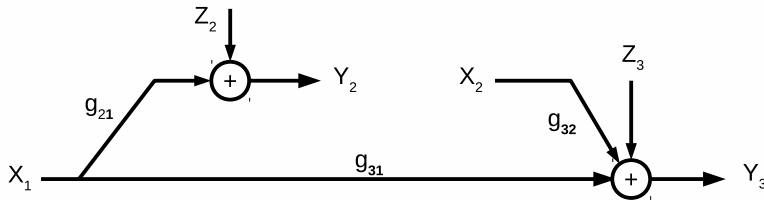
$$Y_2 = g_{21}X_1 + Z_2, \qquad Y_3 = g_{31}X_1 + g_{32}X_2 + Z_3, \tag{10}$$

where g_{21}, g_{31}, and g_{32} are channel gains, and $Z_2 \sim \mathscr{N}(0,1)$ and $Z_3 \sim \mathscr{N}(0,1)$ are independent noise components. Assume average power constraint P on each of X_1 and X_2. Since the relay can both send X_2 and receive Y_2 at the same time, this model is sometimes referred to as the full-duplex Gaussian relay channel.

We denote the SNR of the direct channel by $\gamma_{31} = g_{31}^2 \cdot P$, the SNR of the channel form the source to the relay by $\gamma_{21} = g_{21}^2 \cdot P$, and the SNR of the channel from the relay to the destination by $\gamma_{32} = g_{32}^2 \cdot P$. In fact, for this model the capacity is not known for arbitrary $\gamma_{21}, \gamma_{31}, \gamma_{32} > 0$.

The cutset bound is attained by jointly Gaussian probability distribution function (PDF) of (X_1, X_2) [10, eq.(8.35)]:

$$C \leq \max_{0 \leq \rho \leq 1} \min \left\{ C\left(\gamma_{31} + \gamma_{32} + 2\rho\sqrt{\gamma_{31}\gamma_{32}}\right), C\left(\left(1 - \rho^2\right)\left(\gamma_{31} + \gamma_{21}\right)\right) \right\} . \tag{11}$$

Figure 5: Gaussian Relay Channel

where $\rho = E\left(X_1 X_2\right) / \sqrt{E\left(X_1^2\right) \cdot E\left(X_2^2\right)}$.
Direct-transmission lower bound is:

$$C \geq C\left(\gamma_{31}\right) . \tag{12}$$

For the *cascade* relay channel the distributions on the inputs X_1 and X_2 that optimize the bound are not known in general. Assuming X_1 and X_2 to be Gaussian we obtain the lower bound:

$$C \geq \min\left\{C\left(\gamma_{21}\right), C\left(\gamma_{32}/\left(\gamma_{31}+1\right)\right)\right\} . \tag{13}$$

Maximizing the *decode-and-forward* lower bound in (5) subject to constraints yields:

$$C \geq \max_{0 \leq \rho \leq 1} \min\left\{C\left(\gamma_{31} + \gamma_{32} + 2\rho\sqrt{\gamma_{31}\gamma_{32}}\right), C\left(\left(1-\rho^2\right) \cdot \gamma_{21}\right)\right\} . \tag{14}$$

Since implementing coherent communication is difficult in wireless systems, one may consider a *non-coherent decode-and-forward* relaying scheme, where X_1 and X_2 are independent. In this model the lower bound is:

$$C \geq \min\left\{C\left(\gamma_{31} + \gamma_{32}\right), C\left(\gamma_{21}\right)\right\} . \tag{15}$$

In general, the capacity of *compress-and-forward scheme* for Gaussian relay channel is not known. If we assume $X_1 \sim \mathcal{N}\left(0, P\right)$, $X_2 \sim \mathcal{N}\left(0, P\right)$, and $Z \sim \mathcal{N}\left(0, N\right)$ are jointly independent and $\hat{Y}_2 = Y_2 + Z$ (Fig. 6), and if we introduce this assumption in (8) and optimize by N the lower capacity bound for CF relay channel is:

$$C \geq C\left(\gamma_{31} + \frac{\gamma_{21} \cdot \gamma_{32}}{\gamma_{31} + \gamma_{21} + \gamma_{32} + 1}\right) . \tag{16}$$

CF scheme outperforms the DF scheme when the channel from the source to the destination
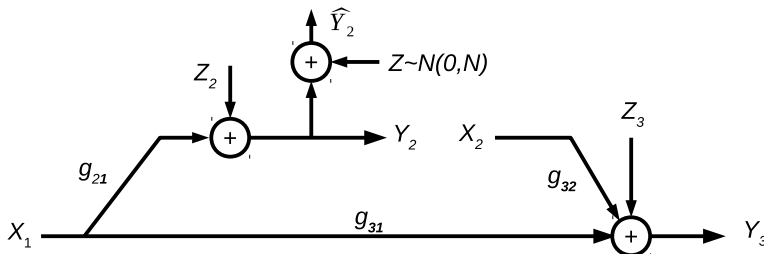
Figure 6: Compress-and-forward for Gaussian relay channel

is worse than the channel from the source to destination i.e. when $\gamma_{21} < \gamma_{31}$, or when the channel from relay to destination is not good. DF scheme shows better results then CF in other scenarios. In general, for both schemes it may be shown that the achievable rates are within half bit of CUB [3, ch.(16.7.2)].
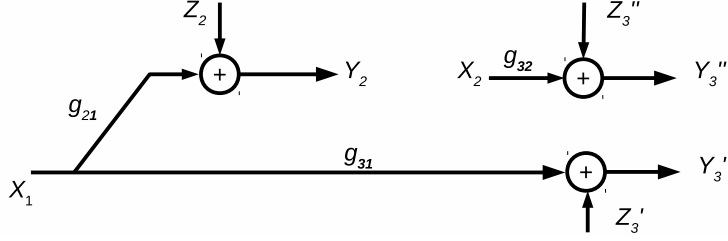
Figure 7: Gaussian channel with frequency division in the destination

The relay channel with receiver frequency division (RFD) at the receiver of destination shown on Fig. 7 is subtype of the ORC relay channel.

In this *half-duplex system*, the channel from the relay to the destination is using different frequency band from the broadcast channel from the source to the relay and destination. More precisely for this model: $Y_3 = (Y_3', Y_3'')$ and

$$Y_2 = g_{21}X_1 + Z_2, \qquad Y_3' = g_{31}X_1 + Z_3' \qquad Y_3'' = g_{32}X_2 + Z_3'', \tag{17}$$

where g_{21}, g_{31}, and g_{32} are channel gains, and $Z_2 \sim \mathcal{N}(0,1)$ and $Z_3 \sim \mathcal{N}(0,1)$ are independent noise components and we assume average power constraint P on X_1 and X_2.

The capacity of this channel is not known in general. Under the power constraints the *CUB* in (1) simplifies to:

$$C \leq \begin{cases} C(\gamma_{31}) + C(\gamma_{32}) & \text{if } \gamma_{21} \geq \gamma_{32}(\gamma_{31} + 1) \\ C(\gamma_{21} + \gamma_{31}) & \text{otherwise} \end{cases}. \tag{18}$$

The *decode-and-forward* lower bound in (5) simplifies to:

$$C \geq \begin{cases} C(\gamma_{31}) + C(\gamma_{32}) & \text{if } \gamma_{21} \geq \gamma_{32}(\gamma_{31} + 1) \\ C(\gamma_{21}) & \text{otherwise} \end{cases}. \tag{19}$$

The *compress-and-forward* lower bound in (8) with $X_1 \sim \mathcal{N}(0,P)$, $X_2 \sim \mathcal{N}(0,P)$ and $Z \sim \mathcal{N}(0,N)$, independent of each other, and $\hat{Y}_2 = Y_2 + Z$, simplifies (after optimizing over N) to:

$$C \geq C\left(\gamma_{31} + \frac{\gamma_{21} \cdot \gamma_{32} \cdot (\gamma_{31} + 1)}{\gamma_{21} + (\gamma_{31} + 1) \cdot (\gamma_{32} + 1)}\right). \tag{20}$$

In case of RFD Gaussian relay channel with *linear relaying* the relaying functions are restricted to being linear combinations of past received symbols. Note that under the ORC assumption, we can eliminate the delay in relay encoding simply by relabeling the transmission time for the channel from X_2 to Y_3''. Hence, we equivalently consider relaying functions of the form $x_{2i} = \sum_{j=1}^{i} a_{ij}y_{2j}$ $i \in [1:n]$ or in vector notation of the form $X_2^n = A \cdot Y_2^n$ where A is and $n \times n$ lower triangular matrix.

$$\begin{bmatrix} x_{21} \\ x_{22} \\ \dots \\ x_{2n} \end{bmatrix} = \begin{bmatrix} a_{11} & 0 & 0 & 0 \\ a_{21} & a_{22} & 0 & 0 \\ \dots & \dots & \dots & \dots \\ a_{n1} & a_{n2} & \dots & a_{nn} \end{bmatrix} \cdot \begin{bmatrix} y_{21} \\ y_{22} \\ \dots \\ y_{23} \end{bmatrix}. \tag{21}$$

This scheme reduces the relay channel to a point-to-point Gaussian channel with input X_1^n and output $Y_3^n = (Y_3'^n, Y_3''^n)$. Note that linear relaying is considerably simpler to implement in practice than DF and CF. It turns out that its performance also compares well with these

more complex schemes under certain high SNR conditions. The capacity with linear relaying, C_L, is characterized by the multi-letter expression:

$$C_L = \lim_{k \to \infty} C_L^{(k)} \qquad C_L^{(k)} = \sup_{F\left(x_1^k\right),A} \frac{1}{k} \cdot I\left(X_1^k; Y_3^k\right) . \tag{22}$$

The supremum is over all cumulative distribution functions (CDFs) $F\left(x_1^k\right)$ and lower triangular matrices A that satisfy the source and the relay power constraint P. It can be shown that $C_L^{(k)}$ is attained by a Gaussian input X_1^k that satisfies the power constraint [3].

If in (22) we consider $C_L^{(1)}$, we obtain the maximum rate achievable via a simple *AF relaying* scheme. By observing the figure Fig. 8 and taking $C_L^{(1)} = I\left(X_1; Y_{31}' Y_{31}''\right)$, it can be shown that $C_L^{(1)}$ is attained by $X_1 \sim \mathcal{N}\left(0, P\right)$ and $X_2 = Y_2 \sqrt{P/\left(\gamma_{21} + 1\right)}$. Therefore:

$$C_L^{(1)} = C\left(\gamma_{31} + \frac{\gamma_{21}\gamma_{32}}{\gamma_{21} + \gamma_{32} + 1}\right) . \tag{23}$$

The model of the AF cascade relay channel is based on the AF Gaussian relay channel given
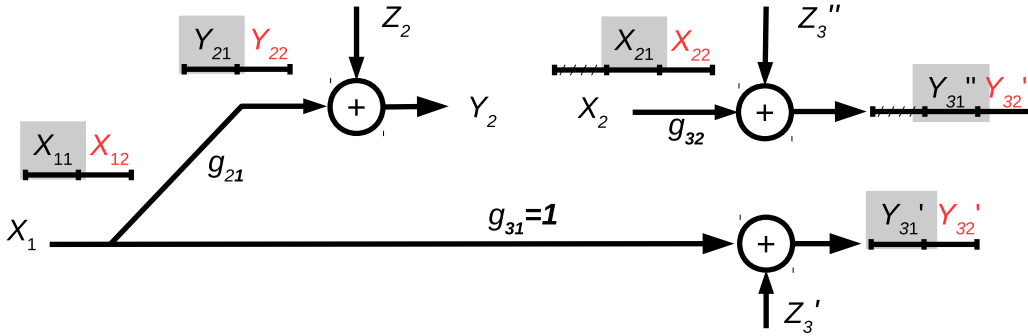
Figure 8: Amplify-and-forward relay channel

on Fig. 8 but without existence of the direct path component from the source to the destination i.e. $g_{31} = 0$. The capacity of this type of channel may be obtained if we take $C_L^{(1)} = I\left(X; Y_3''\right)$ or if in (23) we let $\gamma_{31} = 0$:

$$C_L^{(1)} = C\left(\frac{\gamma_{21}\gamma_{32}}{\gamma_{21} + \gamma_{32} + 1}\right) . \tag{24}$$

2 Performance analysis of AF MIMO relay channels with multiple antennas per node

There is abundance of research papers related to AF MIMO relaying systems. Some focus on single-antenna relays ([15]-[19]) and some on multiple-antenna relays ([5], [20]-[25]). Most of the papers in the literature for the implementation of the MIMO AF relaying system ([5], [17], [18], [21]-[25]) use a specific *amplify-and-forward* (AF) relaying scheme called *Decouple-and-Forward* (DCF) relaying that has recently been proposed by Lee et al. in [5]. DCF is linear processing technique by which the relay converts multiple spatial streams of the received OSTBC signal into a single spatial stream signal without symbol decoding. As a result of this linear decoupling process, if the additive channel noise is neglected, the estimate of the transmitted symbol can be mathematically expressed as product of the transmitted symbol and the sum of the squared modulus of the MIMO channel coefficients. After the relay decouples the OSTBC signal received from the source it re-encodes the decoupled symbols by usage of OSTBC, amplifies each of them separately and transmits them over the relay-destination hop.

In this chapter we study the approximations of the error and outage performance of a dual hop DCF relaying system, consisted of a source, a DCF half-duplex relay and a destination, each equipped with multiple antennas and utilizing an OSTBC transmission technique in a Rayleigh fading environment. We have arrived at a simple universal approximation for the error and outage probability of those systems, which proves to be extremely accurate in the SNR of a practical interest.

2.1 System Model

We analyze the error and outage performance of a dual-hop relay channel (consisted of a source, a relay and a destination), with multiple antennas at the nodes that utilize OSTBC transmission (Fig. 9). We consider two system configurations: $Nx1xN$ configuration, where the source and the destination are equipped with $N_T = N_R = N$ antennas and the relay with single antenna and $NxNxN$ configuration, where the source, relay and destination are each equipped with N antennas. We assume that there is no spatial correlation between the signals transmitted or received in different antennas. The AF relay applies variable-gain amplification of its input signal, which requires the instantaneous channel state information (CSI) of the source-relay hop being available to the relay [26]. The destination is also assumed to have a full CSI of the relay-destination hop for coherent demodulation. In Fig. 9 we present a dual-hop MIMO relay channel (as the most general configuration that incorporates the two system configurations as special cases), where source, relay and destination are denoted by S, R and D, respectively. The relay channel is designated as $Nx1xN$ in the case when the relay has one antenna and $NxNxN$ when the relay has N antennas. The S-R hop and the R-D hop are modeled as the independent MIMO Rayleigh channels with respective channel matrices $\mathbf{H}$ and $\mathbf{G}$. The elements h_{ij} and g_{ij} of these matrices are the channel coefficients between the i-th transmit antenna and j-th receive antenna, considered as independent circularly-symmetric complex Gaussian random processes with zero mean and unit variance. Therefore, the squared envelope of signal transmitted over channel h_{ij} (g_{ij}) follows the exponentially decaying PDF [27] with same mean squared values $E\left[|h_{ij}|^2\right] = E\left[|g_{ij}|^2\right] = 1$. The source average transmit power is P and the direct communication between the source and destination is unavailable. The utilized OSTBC codes are designated as three digit codes, NKL, where N is the number of antennas, K is the number of code symbols transmitted in a code block, and L represents the number of required time slots to transmit a single codeword [28]. For the particular OSTBC the average power per symbol is calculated as:

$$E = P \cdot c, \qquad c = \frac{L}{K \cdot N}. \tag{25}$$

We assume that the communication system operates in half-duplex mode, divided in two phases (phase 1 and phase 2). The source transmits towards the relay during phase 1, then the relay transmits towards the destination during phase 2. Since we assume that the source employs the orthogonal space-time block (OSTB) encoding in the phase 1, group of K information symbols $\mathbf{X} = [x_1, \ x_2, \ ..x_K]^T$ are transmitted over the N transmit antennas in L successive time slots. During the phase 2 the $Nx1xN$ system's relay decouples, amplifies and transmits the K received symbols to the destination. In case of the $NxNxN$ system, during the phase 2 the relay decouples, amplifies, OSTB encodes and transmits the K received symbols to the destination. The received signal in the single relay antenna at the end of the phase 1 is ([29],[30]):

$$\mathbf{Y} = \sqrt{E} \cdot \mathbf{C} \, \mathbf{H} + \mathbf{N} \, , \qquad \mathbf{Y} = [y_1, \ y_2, \ \ldots y_L]^T \, , \tag{26}$$

where $\mathbf{C}$ is LxN codeword matrix of the OSTB code ([28], [31] and [32, eq.(32)]), $\mathbf{H}$ is $Nx1$ channel vector of the S-R hop $\mathbf{H} = [h_1, \ h_2, \ ..h_N]^T$ and $\mathbf{N} = [n_1, \ n_2, \ ..n_L]^T$ is S-R hop's $Lx1$

additive white Gaussian noise (AWGN) vector whose elements have zero mean and variance N_0.
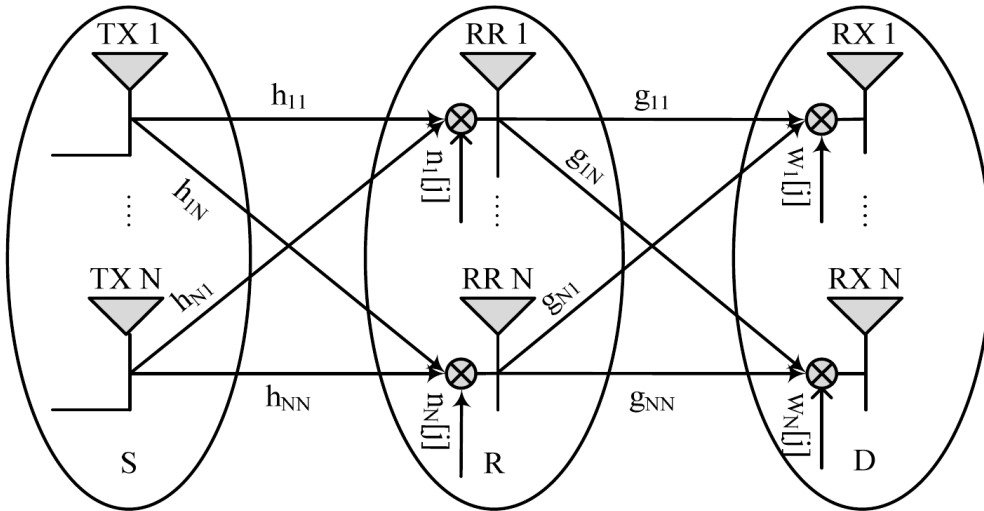
Figure 9: Dual-hop MIMO relay channel

The superscript operator $\mathbf{T}$ denotes matrix transpose operation, and E_S is the average transmitted power per symbol. In [33] it is shown that the particular decoupled symbol at the single antenna at the relay is given by:

$$\tilde{x}_k = \sqrt{E_S} \; \|\mathbf{H}\|_F^2 \; x_k + \xi_k, \quad k = 1, 2, ..K \; , \tag{27}$$

where $\|\mathbf{H}\|_F^2 = \sum_{\mathbf{i=1}}^{\mathbf{N}} |h_i|^2$ is the squared Frobenius norm of the matrix $\mathbf{H}$, ξ is complex-valued AWGN random variable with zero mean and variance $\|\mathbf{H}\|_F^2 \; N_0$. In case where the relay has N antennas (NxNxN system), the decoupled symbol at the relay is again given by (27) where $\|\mathbf{H}\|_F^2 = \sum_{i=1}^{N} \sum_{j=1}^{N} |h_{ij}|^2$. We have chosen to amplify the decoupled symbol $\tilde{x}_k$ with the following amplification factor ([4, eq.(9)], [34], [32, eq.(4)]):

$$A \approx \frac{1}{\sqrt{b} \; \|\mathbf{H}\|_F^2}, \tag{28}$$

where b is the power normalization factor. Namely, in (28) we select $b = c$ for the Nx1xN and $b = 1$ for the NxNxN system. The decision variable for each of the decoupled symbols at the destination is expressed as:

$$\hat{x}_k = A \; \|\mathbf{G}\|_F^2 \; \tilde{x}_k + \mu_k, \quad k = 1, 2, \ldots K, \tag{29}$$

where $\|\mathbf{G}\|_F^2 = \sum_{i=1}^{N} |g_i|^2$ and $\|\mathbf{G}\|_F^2 = \sum_{i=1}^{N} \sum_{j=1}^{N} |g_{ij}|^2$ are the corresponding squared Frobenius norms of the channel matrix $\mathbf{G}$ for the Nx1xN and NxNxN systems, and μ is complex-valued AWGN random variable with zero mean and variance $\|\mathbf{G}\| \cdot N_0$.

In destination the received signal [27] is passed through match filter [35], [36] (since the destination knows the channel coefficients for the R-D hop), after which the destination detects the sent symbols.

2.2 Error Probability

Given that instantaneous channel power for channel h_{ij} follows exponential distribution, the instantaneous SNR of the MIMO channel's hop follows the gamma probability distribution function:

$$f_\Gamma (x) = \frac{x^{\alpha-1}}{\theta^\alpha \cdot \Gamma (\alpha)} \; e^{-\frac{x}{\theta}}. \tag{30}$$

In (30) the scale parameter of the gamma PDF is equal to the average SNR per symbol i.e. $\theta = \overline{\gamma} = E/N_0 = c \cdot \rho = \frac{L}{N \cdot K} \cdot \rho$, where ρ is the total average transmit SNR per symbol. The shape parameter of the gamma PDF given in (30) is $\alpha = m = N$ for the $Nx1xN$ system and $\alpha = m = N^2$ for the $NxNxN$ system.

If we introduce (27) in (29) we obtain the expression that represents the decoupled symbols for both the $Nx1xN$ and $NxNxN$ configurations at the destination:

$$\hat{x}_k = \sqrt{E_s}\, A\, \|\mathbf{H}\|_F^2\, \|\mathbf{G}\|_F^2\, x_k + A\, \|\mathbf{G}\|_F^2\, \xi_k + \mu_k \,. \tag{31}$$

From (31) it is straightforward to express the end-to-end instantaneous signal-to-noise ratio γ. For finding the closed form expression of CDF and PDF for γ it is necessary to calculate the inverse Laplace transform of the MGF for $1/\gamma$ which contain a product of m-th order modified Bessel function of second kind (K_m) ([37, eq.(8.432.1)], [38, eq.(9.6.24)]) with different arguments ([32, eq.(15)], [39], [40]). For larger values of N it is very difficult to find close form expression for the CDF and PDF and finding the average EP with MGF approach given in [27] is even more difficult. Therefore we approximated the function K_m using its power series expansion [37, eq.(8.446)]. For small arguments $z \to 0$, the infinite sum in [37, eq.(8.446)] can be neglected and kept only the finite sum i.e.:

$$K_m(z) \approx \frac{1}{2} \cdot \left(\frac{2}{z}\right)^m \cdot \sum_{k=0}^{m-1} (-1)^k \cdot \frac{(m-k-1)!}{k!} \cdot \left(\frac{z}{2}\right)^{2\,k} \,. \tag{32}$$

By usage of approximation (32) we obtained following closed form expressions of approximate CDF for the $Nx1xN$ and $NxNxN$ systems:

$$
\begin{aligned}
F_{\Gamma_{\mathrm{a}}}(\gamma) \approx 1 + \frac{1}{\Gamma(m)} \cdot \sum_{k=0}^{m-1}\sum_{n=0}^{m-1} \frac{(-1)^{m+k+n}\,\Gamma(m-k)\cdot(2\,k+n-m+1)_{m-n-1}}{\Gamma(m-n)} \\
\cdot \frac{(b+1)^n\,b^k}{\Gamma(k+1)\,\Gamma(n+1)} \cdot \left(\frac{\gamma}{\overline{\gamma}}\right)^{n+2\,k} \cdot \exp\left(-\frac{(b+1)\gamma}{\overline{\gamma}}\right) \,.
\end{aligned}
\tag{33}
$$

where $(...)_{...}$ denotes the Pochhammer symbol. The expression for PDF can easily be found by taking derivate of (33). Based on the approach presented in [41], we used expression (33) to obtain the *tight approximation* of the average EP:

$$
\begin{aligned}
P_{ea} \approx \frac{1}{2} + \frac{\sqrt{d\,\overline{\gamma}}}{2\,\sqrt{\pi}\,\Gamma(m)} \cdot \sum_{k=0}^{m-1}\sum_{n=0}^{m-1} \frac{(-1)^{m+k+n}\,2^{n+2\,k}\,\Gamma(m-k)}{\Gamma(m-n)} \\
\cdot \frac{\Gamma\left(n+2\,k+\frac{1}{2}\right)(2\,k+n-m+1)_{m-n-1}\,(b+1)^n\,b^k}{\Gamma(k+1)\,\Gamma(n+1)\,(d\,\overline{\gamma}+2\,b+2)^{n+2\,k+\frac{1}{2}}} \,,
\end{aligned}
\tag{34}
$$

where d is a constant determined by the modulation and the demodulation scheme (e.g. for BPSK with coherent demodulation $d = 2$).

Based on the approach presented in [42] and by usage of initial value theorem given in [43, eq.(19.1.2.1.9)] the *asymptotic approximation* of average EP for high value SNR range can be presented in the following form:

$$P_{eas} \approx \frac{\Gamma(2\,m+1)\cdot(b^m+1)}{2^{m+1}\cdot\Gamma^2(m+1)\cdot d^m \cdot \overline{\gamma}^m} \,. \tag{35}$$

In order to simplify the mathematical analysis we let $k = 0$ in equation (34), hence we get the *loose approximation* of the average EP for the both system configurations:

$$P_{el} \approx \frac{1}{2} - \frac{\sqrt{d\,\overline{\gamma}}}{2\,\sqrt{\pi}} \cdot \sum_{n=0}^{m-1} \frac{2^n\,\Gamma\left(n+\frac{1}{2}\right)(b+1)^n}{\Gamma(n+1)\,(d\,\overline{\gamma}+2\,b+2)^{n+\frac{1}{2}}} \,. \tag{36}$$

Expressions (33), (34), (35) and (36) can be used for the Nx1xN system by usage of the substitutions: $m = N$ and $b = c$ and for the NxNxN system by usage of the substitutions: $m = N^2$ and $b = 1$.
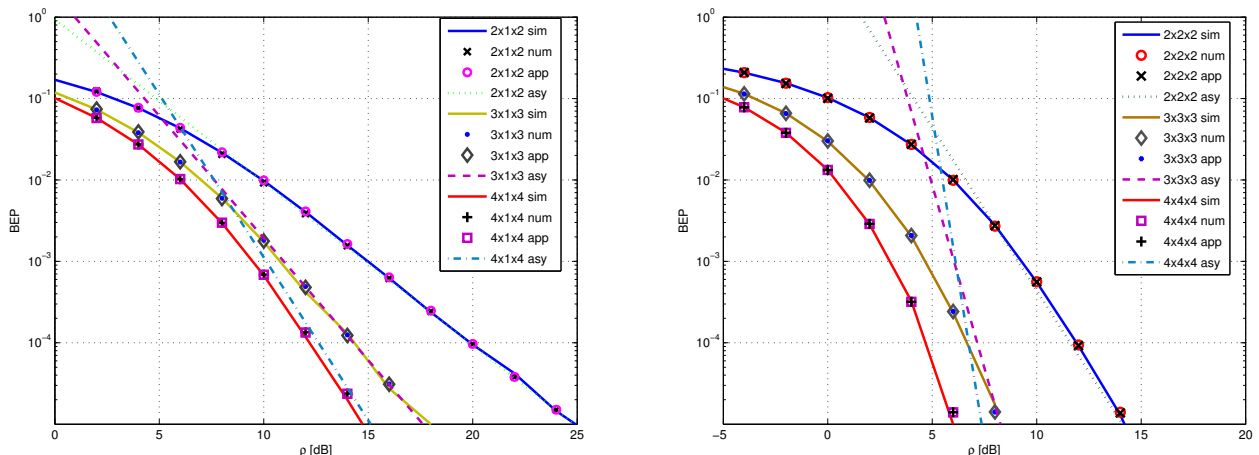
**Figure 10:** BEP for Nx1xN and NxNxN AF relay channel with 222/334/434 OSTBC

On Fig. 10 (left) we present the bit error probability (BEP) ($d = 2$) for 2x1x2 system with Alamouti's coding [44], 3x1x3 with 334 OSTBC and 4x1x4 system with 434 OSTBC ([28], [31] and [32, eq.(32)]). We have compared the results obtained by Monte Carlo simulation, the approximation results obtained by (34) and (35) for $m = N$ and $b = c$ and exact results obtained by numeric integration of [27, eq.(9.15)] by using the expressions for MGF obtained by approach presented in [17]. The comparison has shown close match of the results obtained by approximation (34) and exact result obtained by numerical integration and simulation.

On Fig. 10 (right) we present the BEP for 2x2x2, 3x3x3 and 4x4x4 systems using 222, 334 and 434 OSTBC ([28], [31] and [32, eq.(32)]). On the figure we present a comparison of the results obtained by means of simulation, results obtained by usage of tight EP approximation (34), results obtained by asymptotic EP approximation (35) and results obtained by numeric integration of MGF given in [22, eq.(15)] by usage of [27, eq.(9.15)]. We have chosen to use MGF presented in [22] due to better numerical computational tractability. Again, the comparison has shown close match of the results obtained by approximation (34), numerical integration and simulation.

Henceforth, we are going to illustrate the accuracy of the loose EP approximation (36). We validate its accuracy for different number of antennas N with comparison with: (a) accurate results obtained by numerical integration of appropriate MGF functions, and (b) accurate values obtained with Monte Carlo simulations. We focus on 222, 334 and 434 OSTBC schemes [32, eq.(32)] for the system given in Fig. 9. In the figures we use abbreviation "sim" if the curve is obtained by Monte Carlo simulation, the abbreviation "num" if the curve is obtained by numerical integration of the MGF function, abbreviation "ap1" if curve is obtained by the tight approximation (34) and abbreviation "ap2" if the curve is obtained with loose approximation (36).

On Fig. 11 (left) we present the BEP for 2x1x2 system with Alamouti's coding [44], 3x1x3 with 334 OSTBC and 4x1x4 system with 434 OSTBC. We have compared the results obtained by Monte Carlo simulation, the tight approximation (34), the loose approximation (36) and exact results obtained by numeric integration of [27, eq.(9.15)] by using the expressions for MGF obtained by approach presented in [17]. The comparison shows close match of the results obtained by tight approximation (34), exact result obtained by the numerical integration and
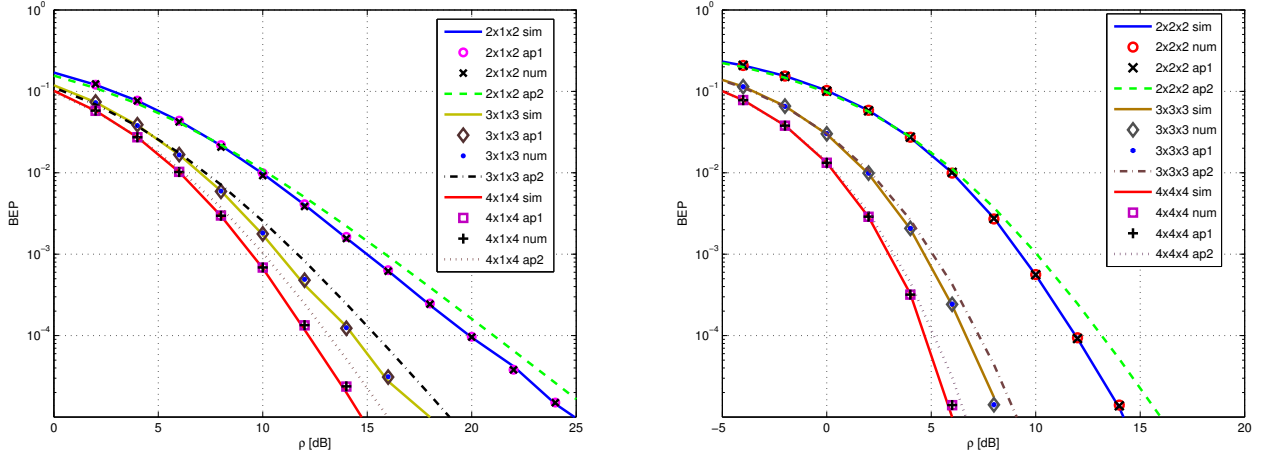
Figure 11: Tight and loose BEP for Nx1xN and NxNxN AF MIMO relay channel with 222/334/434 OSTBC

simulation. Moreover, the comparison shows good matching of the loose approximation (36) and the exact results. On Fig. 11 (right) we present the BEP for 2x2x2, 3x3x3 and 4x4x4 systems using 222, 333 and 434 OSTBC. On the figure we present a comparison of the results obtained by means of simulation, results obtained by usage of tight EP approximation (34), loose EP approximation (36) and results obtained by numeric integration of MGF given in [22, eq.(15)] by usage of [27, eq.(9.15)]. We have chosen to use MGF presented in [22] due to better numerical computational tractability. Again, the comparison has shown close match of the results obtained by tight approximation (34), exact result obtained by the numerical integration and simulation. Moreover, the comparison shows good matching of the loose approximation (36) and the exact results.

With the comparison of the results on Fig. 11 we have shown that the results obtained with the loose EP approximation match very well with the accurate values obtained by simulation, numerical integration and the tight approximation (34). The matching of the results is better for lower values of the SNR range.

2.3 Outage probability

We derived universal OP approximation for the relay channel given on Fig. 9, which is very accurate for entire SNR range of practical interest. Moreover, we simplify the tight approximation in loose form which is more appropriate for further theoretical analysis [45]. OP is defined as probability that instantaneous SNR falls below the threshold γ_{th} (33):

$$P_{\text{out}} = P\left(\gamma < \gamma_{th}\right) = F_\Gamma\left(\gamma\right)|_{\gamma=\gamma_{th}} \approx F_{\Gamma_a}\left(\gamma\right)|_{\gamma=\gamma_{th}}. \tag{37}$$

By introducing of [32, eq.(15)] in [32, eq.(16)] we obtain the accurate values of OP by usage of numeric inversion of Laplace transform and by usage of (37) we obtain the tight OP approximation for the two system configurations (Nx1xN и NxNxN). In order to get the loose approximation we simplified (33) by letting $k = 0$:

$$P_{\text{out}} \approx F_{\Gamma_a}\left(\gamma\right)|_{\gamma=\gamma_{th}} = 1 - \sum_{n=0}^{m-1} \frac{(b+1)^n}{n!} \cdot \left(\frac{\gamma_{th}}{\overline{\gamma}}\right)^n \cdot \exp\left(-\frac{(b+1)\gamma_{th}}{\overline{\gamma}}\right). \tag{38}$$

We use (37) and (38) for calculation of tight and loose approximation of OP for Nx1xN ($m = N$ and $b = c$) and NxNxN ($m = N^2$ and $b = 1$) system .
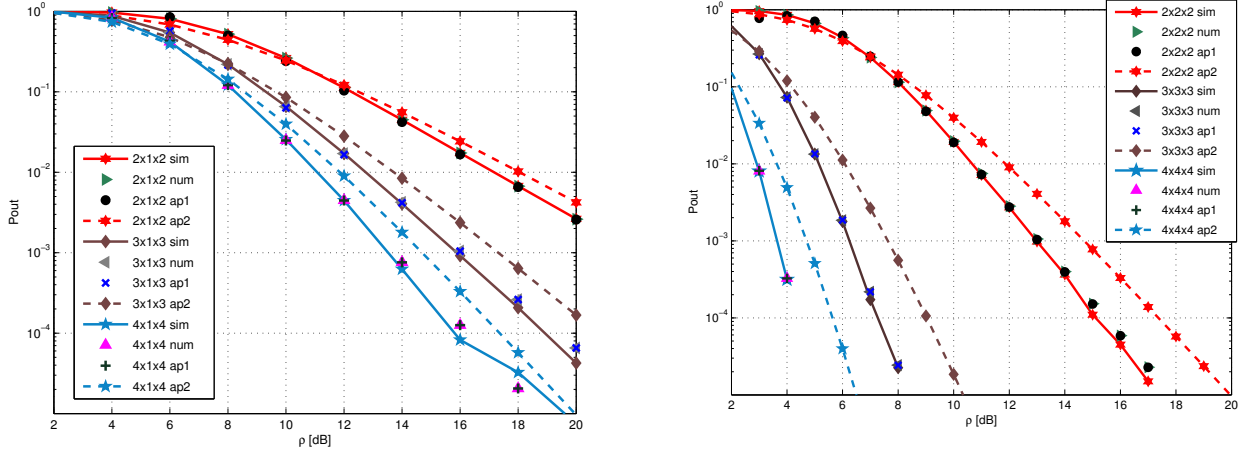
**Figure 12:** OP for AF MIMO relay channel with single and multiple antenna relay($\gamma_{th} = 5dB$).

The results obtained for tight and loose approximation are compared with the accurate results obtained with numerical inversion of Laplace transform of the appropriate MGF and with the results obtained by Monte Carlo simulation. For inverse Laplace transform we used Euler's numerical technique ([46, eq.(12)], [46, eq.(13)]). We focus on 222, 334 и 434 OSTBC schemes. In the figures we use abbreviation "sim" if the curve is obtained by usage of Monte Carlo simulations, the abbreviation "num" if the curve is obtained by numerical integration of the appropriate MGF function, the abbreviation "ap1" if the curve is obtained with tight approximation (37) and abbreviation "ap2" if the curve is obtained by loose approximation (38).

On Fig. 12 (left) we present OP performance results for the Nx1xN system with up to 4 antennas at the source and the destination. The solid line curves represent the OP results obtained by Monte Carlo simulations, the triangle markers represent the exact OP results obtained by numerical inversion of Laplace transform, the dashed line curves represent the results obtained by loose OP approximation (38) and remaining markers (o, x and +) represents the results obtained by the expression for tight OP approximation (37). Similarly, on Fig. 12 (right) we present the OP results for the NxNxN system with up to 4 antennas at the source, relay and destination. The solid line curves represent the OP results obtained by Monte Carlo simulations, the triangle markers represent the exact OP results obtained by numerical inversion of Laplace transform, the dashed line curves represent the results obtained by loose approximation (38) and remaining markers (o, x and +) represents the results obtained by the expression for tight approximation of the outage probability (37). Both comparisons show close match of the results obtained by approximation (37), exact results obtained by the numerical inversion of the Laplace transform and the results obtained by the Monte Carlo simulation. Moreover, the comparison shows good matching of the loose OP approximation (38) and the exact results.

2.4 AF MIMO relay channel: inclusion of direct path in the analysis

In sections 2.2 and 2.3 we have analyzed the performance of the AF MIMO relay channels which don't have direct path from the source to the destination. This type of relay channels are usually called cascade relay channels. Henceforth we are going to expand the analysis by including the direct path from the source to the destination.

From the information-theoretic analysis in chapter 1 it is obvious that usage of the relay which is helping the communication may increase the capacity of the system. If we closely
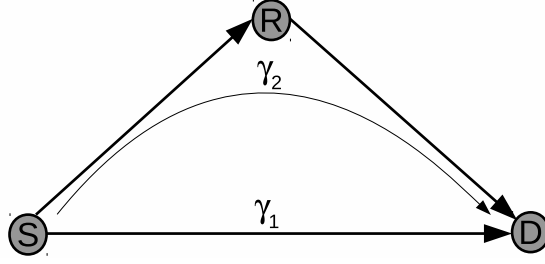
Figure 13: Relay channel with direct path to the destination

analyze the expression for capacity of AF relay channel (23) we see that total instantaneous end-to-end SNR is a sum of two random variables: the instantaneous SNR on the hop from the source to the destination - γ_1 (Fig. 13) and the equivalent instantaneous SNR on the hop which is including the relay - γ_2 (Fig. 13). Henceforth we are going to analyze the performance of this relay channel with assumption that the relay is using AF relaying scheme and that the γ_1 is statistically independent from γ_2.

For the sake of simplified theoretical analysis we are going to simplify the expressions for CDF (33). Accuracy of this approximation is tested for the cascade AF MIMO relay channel through the analysis of the loose BEP approximation in section 2.2 and loose OP approximation in section 2.3. Following the same approach as for obtaining (36) and (38) for simplification of (33) we let $k = 0$. By usage of certain mathematical operations as shown in [47, eq.(16)-eq.(18)] we obtain the loose approximation of the CDF:

$$F_{\Gamma_l}(\gamma) \approx 1 - \frac{\Gamma\left(m, \frac{(b+1)\gamma}{\overline{\gamma}}\right)}{\Gamma(m)} = \frac{\gamma\left(m, \frac{(b+1)\gamma}{\overline{\gamma}}\right)}{\Gamma(m)} \ , \tag{39}$$

where $\Gamma(.)$ is Gamma function [37, eq. (8.310.1)], $\Gamma(.,.)$ is upper incomplete Gamma function [37, eq. (8.350.2)], $\gamma(...)$ is lower incomplete Gamma function [37, eq. (8.350.1)]. CDF function given with (39) is CDF of random variable which follows the Gamma PDF with parameter of shape m and scale parameter $\theta = \overline{\gamma}/(b+1)$, hence the end-to-end instantaneous SNR for the two-hop cascade AF MIMO relay channel may loosely be approximated by random variable which follows Gamma PDF:

$$f(\gamma) = \frac{1}{\theta^m \cdot \Gamma(m)} \gamma^{m-1} e^{-\frac{\gamma}{\theta}} \qquad \text{where } \theta = \frac{\overline{\gamma}}{b+1} \text{ and } \overline{\gamma} = \frac{L}{N_T \cdot K} \cdot \rho. \tag{40}$$

If we assume Rayleigh fading in the direct hop from the source to the destination, the instantaneous SNR of this hop is following the gamma PDF (30) with scale parameter $\theta = \overline{\gamma}$ and shape parameter $\alpha = m$ and the instantaneous SNR of the hop passing via the relay is following (40). The total SNR is a sum of two random variables which follow Gamma PDF with different shape parameters. In the thesis by usage of [48] it is shown that resulting PDF is:

$$f_{\Gamma}(\gamma) = \frac{1}{(b+1)^m} \cdot \sum_{k=0}^{\infty} \frac{(m)_k}{k!} \cdot \left(\frac{b}{b+1}\right)^k \cdot \frac{\gamma^{2m+k-1}(b+1)^{2m+k}}{\Gamma(2m+k) \cdot \overline{\gamma}^{2m+k}} \cdot e^{-\frac{(b+1)\cdot\gamma}{\overline{\gamma}}}. \tag{41}$$

If we replace (41) in (37) we obtain the OP of the AF MIMO relay channel with direct path to the destination:

$$P_{out} = 1 - \frac{1}{(b+1)^m} \cdot \sum_{k=0}^{\infty} \frac{(m)_k}{k!} \cdot \left(\frac{b}{b+1}\right)^k \cdot \frac{\Gamma\left(2m+k, \frac{\gamma_{th}(b+1)}{\overline{\gamma}}\right)}{\Gamma(2m+k)}. \tag{42}$$
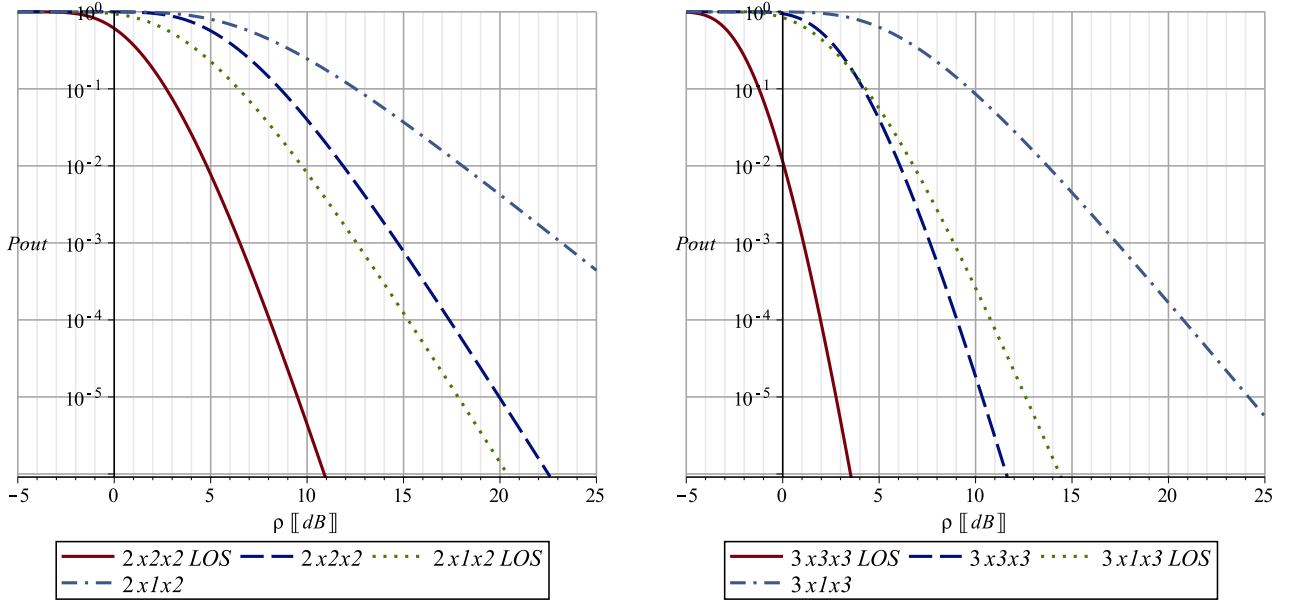
Figure 14: OP for $NxNxN/Nx1xN$ with 222/334 OSTBC relay channel with and without direct path for $\gamma_{th} = 5dB$

We use (42) for calculation of loose approximation of OP for $Nx1xN$ ($m = N$ and $b = c$) and $NxNxN$ ($m = N^2$ and $b = 1$) relay channels with direct path to the destination.

On Fig. 14 we show the OP of AF MIMO relay channel with and without direct path to the destination for threshold $\gamma_{th} = 5dB$. Namely, on this figures we compare the OP obtained by (38) and (42) which are based on the loose approximation of the CDF of a AF cascade MIMO relay channel given with (39). From the figures we may conclude that the AF MIMO relay channel with direct path has significantly better outage performance compared to cascade AF MIMO relay channel, as it could have been assumed from the information-theoretic analysis in chapter 1. For example, for 2x2x2 system for $\rho = 10dB$ the OP of the cascade relay channel is $4 \cdot 10^{-2}$, and the OP of the same system with direct path is $4 \cdot 10^{-6}$ which is four orders of magnitude improvement. Moreover, we may observe that the AF MIMO relay channel with direct path has greater diversity gain [49, eq.(5.2)] compared to the cascade AF MIMO relay channel. The difference in diversity gain is decreasing with increase of the number of antennas.

3 MIMO relay channel from information-theoretic aspect

In chapter 1 we have analyzed OP and EP performance of MIMO relay channels with and without direct path to the destination, and in this part of the thesis we analyze the ergodic capacity (EC) and outage capacity (OC) of the relay MIMO channels which use OSTBC. The EC is:

$$C = E\left[\log_2\left(1 + \gamma\right)\right] \qquad \text{bit/Hz/s} \,. \tag{43}$$

where γ is the instantaneous SNR, and the operator $E\left[...\right]$ designates average per γ. OC is probability that the instantaneous capacity falls bellow the certain threshold - C_{th}:

$$P_{oc} = Pr\left[C \leq C_{th}\right] = \int_0^{C_{th}} f_c\left(C\right) dC \,. \tag{44}$$

15

3.1 Ergodic capacity of cascade AF MIMO relay channel

According (24) the capacity of the AF relay channel without direct path is:

$$C = \frac{1}{2}\log\left(1+\gamma\right) = \frac{1}{2}\log\left(1+\frac{\gamma_{32}\cdot\gamma_{21}}{\gamma_{32}+\gamma_{21}+1}\right). \tag{45}$$

Starting from [32, eq.(8)] it can be shown that the fraction in the logarithm of (45) also represents the end-to-end instantaneous SNR of cascade AF MIMO relay channel.

From other side if we use amplification factor as given in (28) with $b = 1$ the end-to-end instantaneous SNR is:
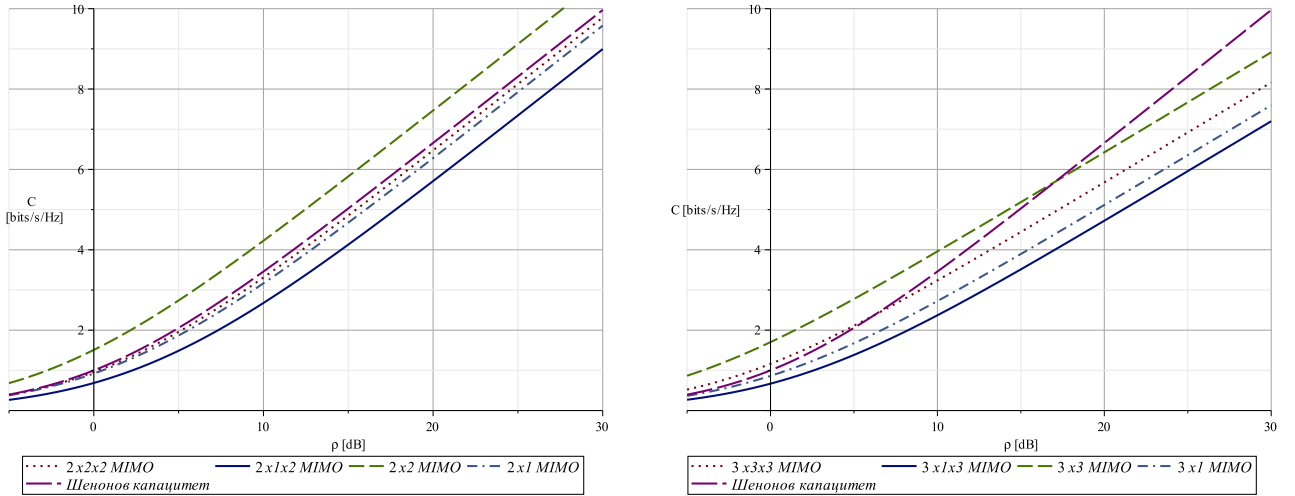
$$\gamma = \frac{\gamma_{31}\cdot\gamma_{32}}{\gamma_{31}+\gamma_{32}} = \frac{L\cdot\rho}{K\cdot N_T}\cdot\frac{\|H\|_F^2\cdot\|G\|_F^2}{\|H\|_F^2+\|G\|_F^2}. \tag{46}$$

Hence the AF MIMO relay channel with OSTBC might be presented with equivalent point-to-point system with ergodic capacity ([50], [51]):

$$C_{AF} = E_H\left\{\frac{K}{L}\cdot\log_2\left(1+\gamma\right)\right\} = E_H\left\{\frac{K}{L}\cdot\log_2\left(1+\frac{\gamma_{32}\cdot\gamma_{21}}{\gamma_{32}+\gamma_{21}+1}\right)\right\} \approx \tag{47}$$

$$\approx E_H\left\{\frac{K}{L}\cdot\log_2\left(1+\frac{\gamma_{32}\cdot\gamma_{21}}{\gamma_{32}+\gamma_{21}}\right)\right\} = E_H\left\{\frac{K}{L}\cdot\log_2\left(1+\frac{L\cdot\rho}{K\cdot N_T}\cdot\frac{\|H\|_F^2\cdot\|G\|_F^2}{\|H\|_F^2+\|G\|_F^2}\right)\right\}. \tag{48}$$

From other side for the AF MIMO relay channel we may use the loose approximation (40)

Figure 15: EC of Nx1xN and NxNxN vs. Nx1 and NxN vs. Shannon capacity for 222 and 334 OSTBC

according which the instantaneous end-to-end SNR of the AF MIMO relay channel is following the Gamma PDF with scale parameter $\theta = \frac{\overline{\gamma}}{b+1}$ where $\overline{\gamma} = \frac{L}{N_T\cdot K}\cdot\rho$ and parameter of shape m. If we introduce (40) in (47) we obtain the ergodic capacity of the cascade AF MIMO relay channel:

$$C_{AF} \approx \frac{K}{L\cdot\Gamma\left(m\right)\cdot\ln\left(2\right)}\cdot G_{3,2}^{1,3}\left(\frac{L\cdot\rho}{K\cdot N_T\cdot\left(b+1\right)}\bigg|_{1,0}^{1-m,1,1}\right), \tag{49}$$

where $G_{3,2}^{1,3}(...)$ is Meijer G function. The equation (49) may be used for Nx1xN if use substitution: $m = N_T$ and $b = c$ and for NxNxN if we change: $m = N_T\cdot N_R = N^2$ и $b = 1$.

On Fig. 15 we compare the approximation of the capacity of AF MIMO relay channel (49) with Shannon capacity [52] and upper bound given by the ergodic capacity of corresponding point-to-point MIMO systems for the two system configurations ($Nx1xN$ and $NxNxN$) in case of 222 and 334 OSTBC. From the figures it is obvious that the approximation (49) is not surpassing the upper bound given by the ergodic capacity of corresponding point-to-point MIMO system and it is approaching the bound by increase of the number of the antennas. Furthermore, the ergodic capacity for $Nx1xN$ system is negligibly lower than the ergodic capacity of the corresponding $Nx1$ point-to-point system and that the difference is increasing by increasing the average SNR and reducing the number of antennas.
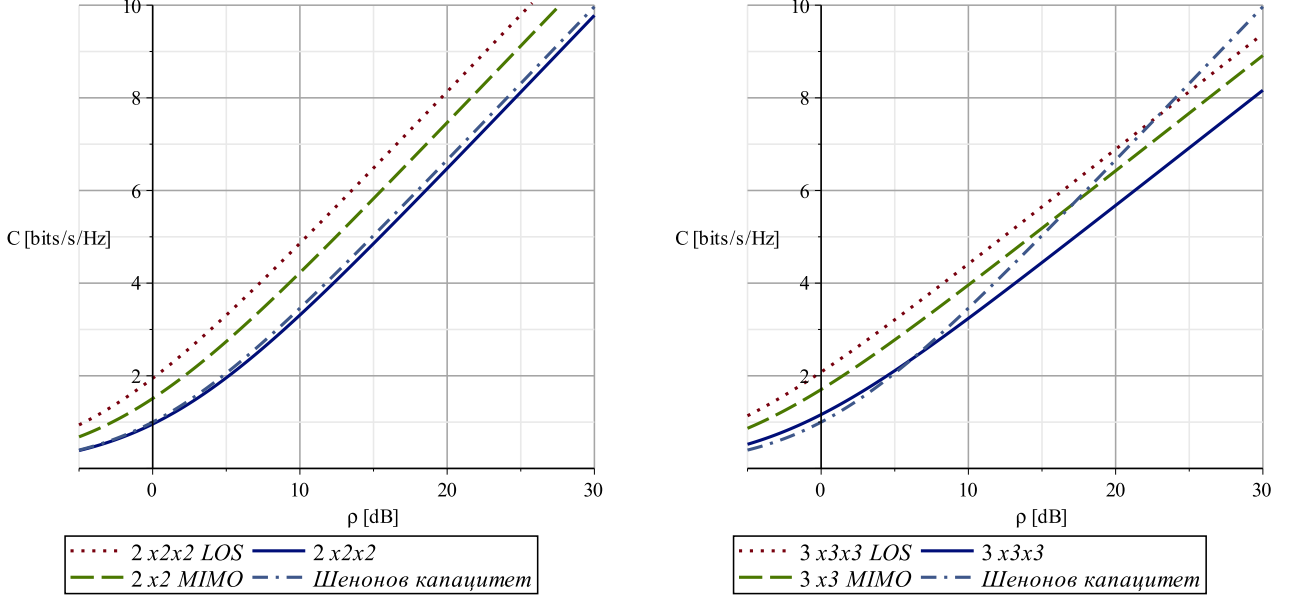
Figure 16: Ergodic capacity for 2x2x2 and 3x3x3 AF MIMO with and without direct path

## 3.2 Ergodic capacity of AF MIMO relay channel with direct path

If (41) is introduced in (47) the ergodic capacity for the AF MIMO relay channel with direct path to the destination is:

$$C_{AF} = \frac{1}{(b+1)^m} \cdot \sum_{k=0}^{\infty} \frac{(m)_k}{k!} \cdot \left(\frac{b}{b+1}\right)^k \cdot \int_0^{\infty} \frac{\gamma^{2m+k-1}(b+1)^{2m+k}}{\Gamma(2m+k) \cdot \overline{\gamma}^{2m+k}} \cdot e^{-\frac{(b+1)\cdot\gamma}{\overline{\gamma}}} \cdot \frac{K}{L} \cdot \log_2(1+\gamma)\, d\gamma.$$

(50)

Without lost of generality in the numerical analysis for AF MIMO relay channel with direct path we focus only on $NxNxN$ system configuration ($m = N_T \cdot N_R = N^2$ и $b = 1$). However (50) might be used for computation of ergodic capacity for $Nx1xN$ system configuration if we use substitutions: $m = N_T$ and $b = c = L/(N \cdot K)$. On Fig. 16 we observe that the system with direct path outperforms the cascade system. Moreover the system with direct path has better performance than point-to-point MIMO system with corresponding number of antennas. The system with direct path do better than Shannon capacity for practical values of the average SNR. The two-antenna system do better then Shannon capacity for whole range of the average SNR, and the other systems has lower capacity than Shannon limit only for the very large values of the average SNR. With increase of the number of antennas the intersection point is shifting to right.

3.3 Outage capacity of cascade AF MIMO relay channel

For calculation of the OP of AF MIMO relay channel, the relay channel is treated as point-to-point channel in which end-to-end instantaneous SNR is following (40).
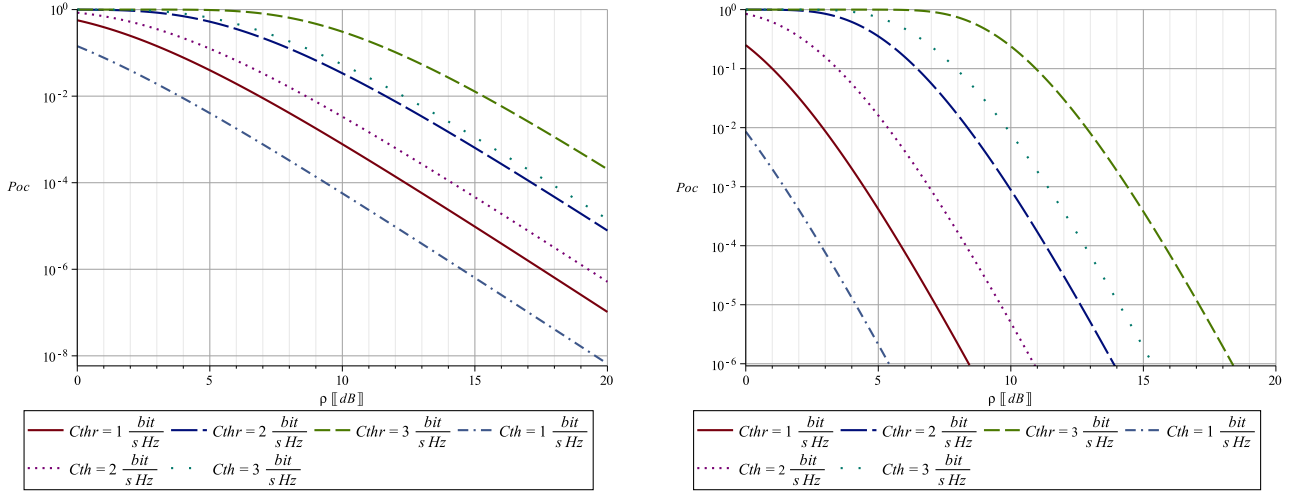
Figure 17: Comparison of the OP for NxN and NxNxN MIMO with 222 and 334 OSTBC for fixed C_{th}

By functional transformation of random variables we can obtain PDF of the instantaneous capacity $C = (K/L) \cdot \log_2 (1 + \gamma)$. Then by usage of (44) we can obtain the OP for AF MIMO OSTBC in Rayleigh fading:

$$P_{oc} = Pr\left(C \leq C_{th}\right) = 1 - \frac{1}{\Gamma(m)} \cdot \Gamma\left(m, \frac{\left(2^{\frac{L \cdot C_{th}}{K}} - 1\right)}{\rho \cdot L} \cdot N_T \cdot K \cdot (b+1)\right). \tag{51}$$

Without lost in generality we have analyzed the NxNxN system configuration ($m = N_T \cdot N_R = N^2$ и $b = 1$), although (51) might be used for computation of OP of Nx1xN system configuration. On Fig. 17 (left) we present the comparison of OP for 2x2 point-to-point and 2x2x2 AF MIMO relay channel with 222 OSTBC for different values of the threshold - C_{th}. The curves with solid and dashed lines are related to the relay channel[1], and the dotted curves are related to the point-to-point system. It is obvious that the relay channel shows worse performance compared to point-to-point system. The performance gap is increased with lowering the threshold C_{th} and increasing the total average SNR - ρ. Note that for small values of the average SNR the performance of the relay channel is approaching the performance of the point-to-point system. By usage of [49, eq.(5.2)] we obtain that the 2x2x2 AF MIMO relay channel has same diversity gain as 2x2 point-to-point MIMO system. On Fig. 17 (right) we compare the OP for 3x3 and 3x3x3 MIMO with 334 OSTBC for different values of the threshold - C_{th}. The difference in the performance is increasing by lowering the threshold C_{th} and by increasing of the total average SNR - ρ. By usage of [49, eq.(5.2)] we can conclude that the 3x3x3 AF MIMO relay channel has same diversity gain as 3x3 point-to-point MIMO system.

If we compare 2x2x2 and 3x3x3 system, besides that 3x3x3 system is using 3/4 code rate it has better performance than 2x2x2 system. For example for $C_{th} = 1\,b/s/Hz$ and $\rho = 5dB$ the OP for 2x2x2 is 0.039 and for 3x3x3 it is $4 \cdot 10^{-4}$ that is almost two order of magnitude better performance. Moreover by usage of [49, eq.(5.2)] we show that diversity gain of 3x3x3 system is $d = 9$, more than twice larger than the diversity gain of 2x2x2 system ($d = 4$).

---

[1]The designation of the threshold variable C_{th} contains additional index „r", i.e. C_{thr}.

3.4 Outage capacity of AF MIMO relay channel with direct path

For calculation of the OC of the AF MIMO relay channel with direct path to the destination (Fig. 13) we assume that end-to-end instantaneous SNR is following the PDF given in (41). By functional transformation of random variables we can obtain PDF of the instantaneous capacity $C = (K/L) \cdot \log_2 (1 + \gamma)$. Then by usage of (44) we can obtain the OP for AF MIMO relay channel with OSTBC in Rayleigh fading:

$$P_{oc} = 1 - \frac{1}{(b+1)^m} \cdot \sum_{k=0}^{\infty} \frac{(m)_k}{k!} \cdot \left(\frac{b}{b+1} \right)^k \cdot \frac{1}{\Gamma(2m+k)} \Gamma \left(2m+k, \frac{2^{\frac{LC_{th}}{K}} - 1}{\overline{\gamma}} \cdot (b+1) \right) . \quad (52)$$

Without lost of generality in numerical analysis of the AF MIMO relay channel with direct
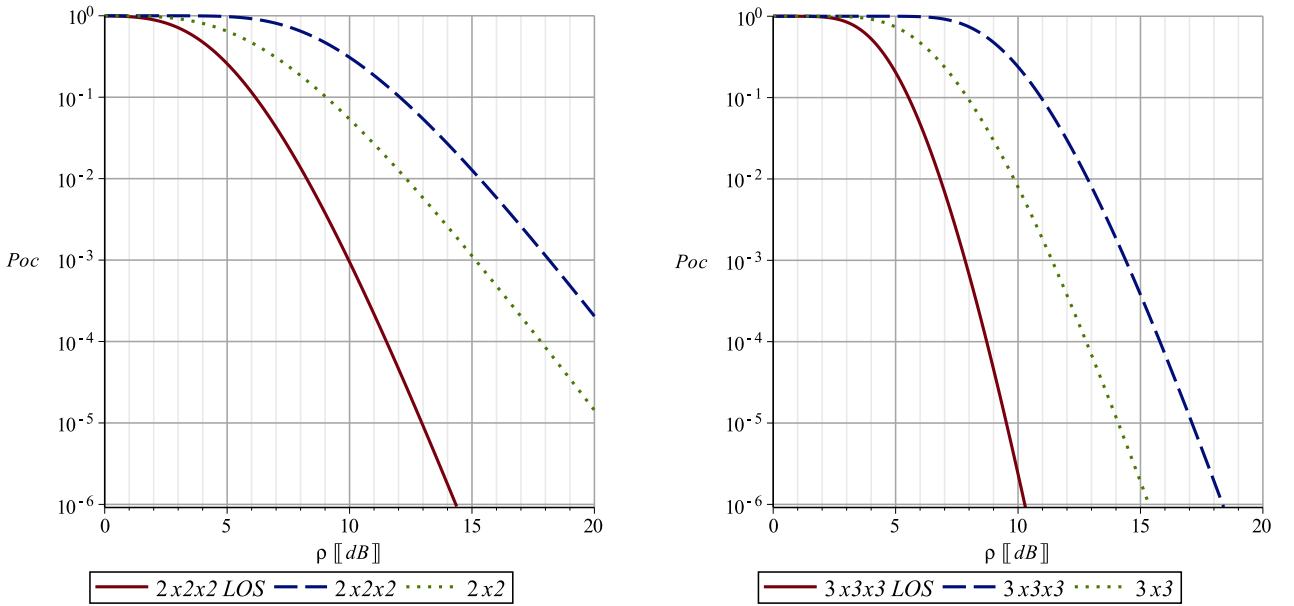
Figure 18: OP for 2x2x2 and 3x3x3 AF MIMO relay channel with and without direct path for $C_{th} = 3 bit/s/Hz$

path we focus on NxNxN system configuration ($m = N_T \cdot N_R = N^2$ и $b = 1$), although (52) might be used for Nx1xN system configuration if we use substitutions: $m = N_T$ и $b = c = L/(N \cdot K)$. On Fig. 18 we compare OC for 2x2x2 and 3x3x3 AF MIMO relay channel with (52) and without (51) direct path and corresponding point-to-point MIMO systems. We observe that the systems with direct path have significantly better OC performance than the cascade AF MIMO relay channel and point-to-point systems. Moreover the systems with direct path show grater diversity gain.

References

[1] A. Sendonaris, E. Erkip, B. Aazhang, "User Cooperation Diversity Part I and Part II," *IEEE Transactions on Communications,* vol. 51, no. 11, pp. 1927-48, 2003.

[2] T. M. Cover, A. E. Gamal, "Capacity Theorem for the relay channels," *IEEE Transactions on Information Theory*, vol. IT-25, no. 5, September 1979.

[3] A. E. Gamal, Y-H. Kim, *Network Information Theory*, Cambridge University Press, 2011.

[4] J. N. Laneman, D. N. C. Tse, "Cooperative Diversity in Wireless Networks Efficient Protocols and Outage Behavior," *IEEE Transactions on Information Theory*, vol. 50, no. 12, December 2004

[5] I-H. Lee, D. Kim, "Decouple-and-Forward Relaying for Dual-Hop Alamouti Transmissions," *IEEE Communications Letters,* No.2, 2008.

[6] E. C. van der Meulen, "Three-terminal communication channels," *Adv. Appl. Prob.*, vol. 3, pp. 120-154, 1971.

[7] A. E. Gamal and M. Aref, "The capacity of the semideterministic relay channel," *IEEE Trans. Inform. Theory*, vol. IT-28, no. 3, p. 536, May 1982.

[8] A. E. Gamal and S. Zahedi, "Capacity of a class of relay channels with orthogonal components," IEEE Trans. Inform. Theory, vol. 51, no. 5, pp. 1815–1817, May 2005.

[9] T. M. Cover, "Capacity of a class of deterministic relay channels," *Proc. IEEE Int. Symp. Information Theory*, Nice, France, June 24–29, 2007.

[10] T. M. Cover, J. A. Thomas, *Elements of Information Theory*, Second Edition, John Wiley & Sons, 2006.

[11] L. R. Ford, D. R. Fulkerson, *Flows in Networks, Princeton*, NJ: Princeton Univ. Press, 1962.

[12] T. M. Cover, C. S. K. Leung, "An achievable rate region for mutiple-access channel with Feedback," *IEEE Transactions on Information Theory*, vol. IT-27, no. 3, May 1981.

[13] D. Slepian, J. K. Wolf, "Noiseless coding of correlated information sources," *IEEE Trans. Inf. Theory*, vol. IT-19, pp. 471–480, 1973.

[14] A. D. Wyner, "On source coding with side information at the decoder," *IEEE Trans. Inform. Theory*, vol. IT-21, pp. 294-300, May 1975.

[15] Z. Yi, I-M. Kim, Approximate BER Expressions of Distributed Alamouti's Code in Dissimilar Cooperative Networks with Blind Relays, *IEEE Transactions on Communications,* no. 12, 2009.

[16] S. Chen, W. Wang, X. Zhang, Z. Sun, "Performance Analysis of OSTBC Transmission in Amplify-and-Forward Cooperative Relay Networks," *IEEE Transactions on Vehicular Technology*, no.1, 2010.

[17] I-H. Lee, D. Kim, "End-to-End BER Analysis for Dual-Hop OSTBC Transmissions over Rayleigh Fading Channels," *IEEE Transactions on Communications*, no. 3, 2008.

[18] T. Q. Duong, H. J. Zepernick, T. A. Tsiftsis, "Amplify-and-Forward MIMO Relaying with OSTBC over Nakagami-m Fading Channels," IEEE International Conference on Communications, 2010;

[19] I. H. Lee, D. Kim, "End-to-End BER Analysis for Dual-Hop OSTBC Transmissions over Rayleigh Fading Channels," *IEEE Transactions On Communications*, vol. 56, no. 3, March 2008

[20] I. H. Lee, D. Kim, "Decouple-and-Forward Relaying for Dual-Hop Alamouti Transmissions," *IEEE Communications Letters*, vol. 12, no. 2, February 2008.

[21] I-H. Lee, D. Kim, "Achieving Maximum Spatial Diversity with Decouple-and-Forward Relaying in Dual-Hop OSTBC Transmissions," *IEEE Transactions on Wireless Communications*, no. 3, 2010.

[22] L. Yang, Q. T. Zhang "Performance Analysis of MIMO Relay Wireless Networks With Orthogonal STBC," *IEEE Transactions on Vehicular Technology*, no. 7, pp. 3668-74, 2010.

[23] Y. Chen, G. Wu, W. Lin, Q. Li, S. Li, "Outage Probability of Space-Time Coded Decouple-and-Forward Relaying over Nakagami-m Fading Channels," *International Conference on Wireless Communications, Networking and Mobile Computing,* 2009.

[24] A. Abdaoui, M. H. Ahmed, "On the Performance Analysis of a MIMO-Relaying Scheme With Space-Time Block Codes," IEEE Transactions On Vehicular Technology, no. 7, 2010.

[25] P. Dharmawansa, M. R. McKay, R. K. Mallik, Analytical Performance of Amplify-and-Forward MIMO Relaying with Orthogonal Space-Time Block Codes, *IEEE Transactions on Communications*, no. 7, 2010.

[26] M. O. Hasna, M. S. Alouini, "A Performance Study of Dual-Hop Transmissions With Fixed Gain Relays," IEEE Transactions On Wireless Communications, Vol.3, no. 6, 2004.

[27] M. K. Simon, M. S. Alouini, *Digital Communication over Fading Channels*, Second Edition. New York: Wiley, 2005.

[28] H. Jafarkhani, *Space Time Coding Theory and Practice*, Cambridge University Press, 2005.

[29] J. Stosic, Z. Hadzi-Velkov, "Performance analysis of dual-hop MIMO systems", *Proc. 2nd Conference on Information and Communication Technologies' Innovations (ICT Innovations 2010)*, Ohrid, Macedonia, 12-15 September 2010.

[30] J. Stosic, Z. Hadzi-Velkov, "Performance analysis of dual-hop dual-antennas MIMO systems in Rayleigh fading," *Proc. 2nd International Congress on Ultra Modern Telecommunications and Control Systems (ICUMT 2010)*, Moscow, Russia, 18-20 October 2010

[31] V. Tarokh, H. Jafarkhani, A. R. Calderbank, "Space-time block codes from orthogonal designs," *IEEE Transactions On Information Theory*, vol. 5, pp. 1456-67, 1999.

[32] J. Stosic, Z. Hadzi-Velkov, "Simple tight approximations of the error performance for dual-hop MIMO relay systems in Rayleigh fading," *AEÜ - International Journal of Electronics and Communications,* vol. 67, no. 10, pp. 854-960, October 2013.

[33] V. Tarokh, H. Jafarkhani, A. R. Calderbank, "Space-time block coding for wireless communications: Performance results," *IEEE Journal on Selected Areas in Communications*, no.3, pp. 451-60, 1999.

[34] J. N. Laneman, G. W. Wornell, "Energy efficient antenna sharing and relaying for wireless networks," *Proc. IEEE Wireless Communications Networking Conf.*, Chicago, IL, Oct. 2000.

[35] J. Proakis, *Digital Communications*, 4 edition, McGraw-Hill, August 2000.

[36] B. Sklar, *Digital Communications: Fundamentals and Applications*, Second Edition, Prentice Hall, January 2001.

[37] I. S. Gradshteyn, I. M. Ryzhik, *Table of Integrals, Series, and Products*, 6th edition, Academic Press, 2000.

[38] M. Abramowitz, I. A. Stegun, *Handbook of Mathematical Functions with Formulas, Graphs, and Mathematical Tables*, 9th edition, New York: Dover, 1970.

[39] M. O. Hasna, M. S. Alouini, "End-to-End Performance of Transmission Systems With Relays Over Rayleigh-Fading Channels," *IEEE Transactions on Wireless Communications*, no. 6, 2003.

[40] A. P. Prudnikov, A. Brychkov, O. I. Marichev, *Integrals and Series Volume 4: Direct Laplace Transforms*, Gordon And Breach Science Publishers, 1992.

[41] Y. Zhao, R. Adve, T. J. Lim "Symbol error rate of selection amplify-and-forward relay systems," IEEE Communications Letters, no. 11, 2006.

[42] P. A. Anghel, M. Kaveh, "On the Performance of Distributed Space-Time Coding Systems with One and Two Non-Regenerative Relays," *IEEE Transactions On Wireless Communications*, vol. 3, 2006.

[43] A. Jeffrey, H. H. Dai, *Handbook of Mathematical Formulas and Integrals*, Fourth Ehdition, Academic Press, 2008.

[44] S. M. Alamouti, "A Simple Transmit Diversity Technique for Wireless Communications," *IEEE Journal on Select Areas in Communications*, vol. 16, no. 8, October 1998.

[45] J. Stosic, Z. Hadzi-Velkov, "Outage probability approximations for dual-hop Amplify-and-Forward MIMO relay systems in Rayleigh fading", Proc. 11th International Conference on Telecommunication in Modern Satellite, Cable and Broadcasting Services (TELSIKS 2013), Nis, Serbia, 16-19 October 2013.

[46] J. Stosic, Z. Hadzi-Velkov, "Outage Probability of Multi-hop Relay Systems in Various Fading Channels," *Proc. 1st Conference on Information and Communication Technologies' Innovations (ICT Innovations 2009)*, 27-30 September 2009.

[47] J. Stosic, and Z. Hadzi-Velkov, "Approximate Performance Analysis of Dual-hop Decouple-and-Forward MIMO Relaying," *Proc. 11th International Conference on Electronics, Telecommunications, Automation and Informatics (ETAI 2013)*, Ohrid, Macedonia, 26-28 September 2013.

[48] P. G. Moschopoulos, "The Distribution of the Sum of Independent Gamma Random Variables," *Annals of the Institute of Statistical Mathematics*, 1985.

[49] G. Kramer, I. Maric, and R. D. Yates, *Cooperative Communications (Foundations and Trends in Networking)*, Hanover MA: Now Publishers Inc., 2006.

[50] G. J. Foschini, M. J. Gans, "On Limits of Wireless Communications in Fading Environments when Using Multiple Antennas", *Wireless Personal Communications*, vol. 6, pp. 311-335, March 1998.

[51] I. Telatar, "Capacity of multi-antenna gaussian channels," *AT&T Technical Memorandum*, 1995.

[52] C. E. Shannon, "A mathematical theory of communication," Bell Syst. Tech. J., vol. 27, pp. 379-423, July 1948.